Thermodynamic instability and off-critical slowing down in supersaturated lysozyme solutions

2004 J. Phys.: Condens. Matter 16 S5023

(http://iopscience.iop.org/0953-8984/16/42/017)

INSTITUTE OF PHYSICS PUBLISHING JOURNAL OF PHYSICS: CONDENSED MATTER

J. Phys.: Condens. Matter **16** (2004) S5023–S5033 PII: S0953-8984(04)79038-4

Thermodynamic instability and off-critical slowing down in supersaturated lysozyme solutions

M Manno, D Bulone, V Martorana and P L San Biagio

Italian National Research Council, Institute of Biophysics at Palermo, via Ugo La Malfa 153, I-90146 Palermo, Italy

E-mail: mauro.manno@pa.ibf.cnr.it

Received 6 April 2004
Published 8 October 2004
Online at stacks.iop.org/JPhysCM/16/S5023
doi:10.1088/0953-8984/16/42/017

Abstract

Experimental determination of stability conditions or instability boundaries in protein solution is a powerful tool for testing interaction models and for use in seeking an understanding of the mechanisms leading to protein aggregation. In a recent work on lysozyme solutions at different NaCl concentrations, we have determined the instability boundaries (spinodal line) of a liquid–liquid phase separation, metastable with respect to crystallization. Here, we review previous results, pointing out the scaling critical behaviour of isothermal compressibility with respect to spinodal temperatures, and discuss interaction models and the addition of an entropic term. The measured slowing down of concentration fluctuation dynamics is clearly related to the divergence of the fluctuation correlation length on approaching each point of the spinodal line. This observed off-critical slowing down calls for a crucial role for enhanced fluctuations in the crystallization process.

1. Introduction

Interactions among proteins in solution are a central issue in understanding the mechanisms involved in biologically and technologically relevant aggregation processes, such as protein coagulation and crystallization [1]. An existing powerful tool for studying protein interactions consists in determining the thermodynamic conditions in which a homogeneous protein solution is in stable equilibrium. The phase boundaries depend on molecular interactions; thus an experimental determination of the phase diagram can be used to test any theoretical model [2, 3].

An important example of such an approach has been given by the work on colloids [4–7]. These studies have revealed the crucial role of short range interactions in determining solid–liquid and liquid–liquid coexistence. Such studies have pointed out that the range of attraction between colloids in solution may be the basic parameter in the determination of the phase

diagram. Experimental and theoretical studies have shown that on reducing the range of the attraction potential the liquid–liquid phase transition becomes metastable with respect to the solid–liquid coexistence [8–11].

The model of short range interactions has also been used to explain some experimental results concerning protein crystallization, such as the so-called crystallization slot [12]—the feature that many proteins crystallize when their second virial coefficient lies in a narrow range of (slightly negative) values [9]. This has given a deeper understanding of the classical (semiempirical) recipes, where proteins are crystallized by adding salts in order to screen electrostatic interactions [1].

Since the first work by Ishimoto and Tanaka [13] on lysozyme solutions, the existence of a liquid–liquid coexistence in protein solutions, sometimes metastable with respect to crystallization, has been found in several cases [14–25].

In addition, knowledge of phase diagram is not only a powerful tool for use in interaction modelling, but also an important step towards understanding the overall process of protein aggregation. In fact, liquid–liquid metastable phase transitions affect the kinetics of protein association [26], by altering crystal nucleation rates in the region of liquid–liquid stability [27–30] or by preceding crystallization with nucleation or spinodal demixing [31–34].

In a previous work [25], we studied the thermodynamic stability of lysozyme solutions at various NaCl concentrations, in conditions where liquid–liquid phase separation is metastable with respect to solid–liquid phase separation. By means of static and dynamic light scattering experiments we determined the spinodal line, which is the boundary of thermodynamic instability. These data have been explained by a model in which short range interactions are accompanied by a perturbative term, that could involve long range interactions, hydration forces or hydrophobic effects, according to other experimental results on lysozyme solutions [20, 22]. Also, we have studied experimentally the behaviour of concentration fluctuations on approaching instability.

In this paper, we review previous results and give a discussion of other possible interaction models. Also, we clearly show that both the amplitude and the correlation length of concentration fluctuations exhibit a critical divergent behaviour at off-critical protein concentrations—that is, not only with respect to a second-order phase transition (critical point), but also with respect to any limit of stability (spinodal point) [2, 35]. In the present work, we clarify how to deal with the relaxation rate of fluctuations even in a region not so close to the thermodynamic instability, by working through previous hints from [25]. The observation of an off-critical slowing down of fluctuation in such conditions is the starting point for addressing the role of fluctuations in the crystallization process. In fact, simulations and theoretical studies have shown that critical concentration fluctuations near the critical point may reduce the free energy barrier for crystal nucleation [36–38]. We show that in lysozyme solutions off-critical fluctuations also have a 'critical' behaviour. This suggests that they could have a critical role in crystallization kinetics at off-critical concentrations, and prompts further experimental work.

2. Experimental methods

Hen egg-white lysozyme (from Sigma Chemical Co) and NaCl at the desired volume fractions were dissolved in buffer (0.1 M sodium acetate/acetic acid in Millipore SuperQ water, pH 4.5), centrifuged (8000 g, 10 min) and filtered (0.22 μm filter) into experimental cells. The final concentration was determined by absorption spectroscopy at 280 nm [39].

Static and dynamic light scattering experiments were performed with a Brookhaven BI-9000 correlator and a 100 mW Ar laser tuned at $\lambda_0 = 514.5$ nm. Static scattering experiments can be used to determine the isothermal compressibility κ_T which is proportional to the zero-

angle scattering intensity $I(0)$: $k_T = I(0)/(k_B T I_0 H)$ where k_B is the Boltzmann constant, I_0 is a constant related to experimental conditions and H is a constant related to sample properties (medium refractive index $\tilde{n}$ and mass concentration) [40]. Our experiments were mainly done at an angle $\theta = 90°$, that is at a scattering vector $q = 4\pi\tilde{n}\lambda_0^{-1}\sin(\theta/2) = 0.023\ \mathrm{nm}^{-1}$. The intensity scattered at non-zero scattering vector gives a good measures of $I(0)$, provided that $q\xi < 1$, where ξ is the size or correlation length of scattering objects or fluctuations.

In the same experiment, the intensity autocorrelation function $g_2(t)$ was measured. It was well fitted by a single-exponential function: $g_2(t) = 1 + |A\exp(-\Gamma t)|^2$, where Γ is the correlation (or relaxation) rate, related to the diffusion of single Brownian molecules or local concentration fluctuations.

In a typical experiment, the temperature was scanned downwards at a constant rate (between 3 and 5 °C h^{-1}), and controlled within 0.05 °C. The initial temperature differed depending on the salt and protein concentration; it was chosen to be well above the temperature of thermodynamic instability (or even metastability). During the scanning, simultaneous static and dynamic light scattering measurements were performed. At a given temperature the sample reaches the onset of liquid–liquid phase separation. Due to the formation of regions of different local concentration the sample becomes turbid (cloud point), and further scattering measurements are not possible. This is also a method for measuring the onset of a metastable region (binodal line); see [25] for further details. The results discussed in this paper are related to a homogeneous solution which is stable with respect to liquid–liquid separation. We note that our samples are not stable with respect to crystal formation; indeed, experiments last for a time which is smaller than the nucleation time.

3. Limit of stability: spinodal line

In each downward temperature scanning the scattered intensity, and hence the isothermal compressibility, was found to increase and to exhibit a power law diverging behaviour with respect to a given temperature $T_s(\phi)$. The experimental data can be scaled as in figure 1 by introducing a reduced temperature $\epsilon = T/T_s - 1$:

$$\kappa_T = \kappa_0 \epsilon^{-\gamma} \tag{1}$$

where κ_0 is a constant amplitude parameter and the exponent is $\gamma = 1$.

The latter property provides an experimental method for extrapolating the divergence of the compressibility and for identifying for each volume fraction the spinodal temperature, which is the limit of stability for a homogeneous solution. Indeed, the boundary of thermodynamic stability (spinodal line) is defined by the zero value of one of the free energy second derivatives; thus, one of these conditions can be expressed in terms of the divergence of the isothermal compressibility [41]: $\kappa_T^{-1} = 0$. However, as recalled in section 2, the spinodal temperature is experimentally inaccessible since it is hidden below the coexistence temperature (cloud point). Therefore, it is remarkable that we were able to identify a regular divergent behaviour of compressibility, and determine the spinodal temperature T_s by extrapolation.

This power law behaviour is reminiscent of what is expected along the critical isochore—that is, when approaching a second-order phase transition [42]. The scaling behaviour of a thermodynamic quantity with respect to the critical point can be extended to an analogous scaling along any isochore with respect to the spinodal temperature, according to the so-called 'pseudospinodal hypothesis' [35]. Although the concept of a pseudospinodal deserves more study, as also does clarification of whether it actually coincides with the limit of stability [2], the method has been applied to various liquid systems such as binary mixtures [43, 44] proteins [13, 23–25] and other biopolymeric solutions [45], by using an experimental set-up

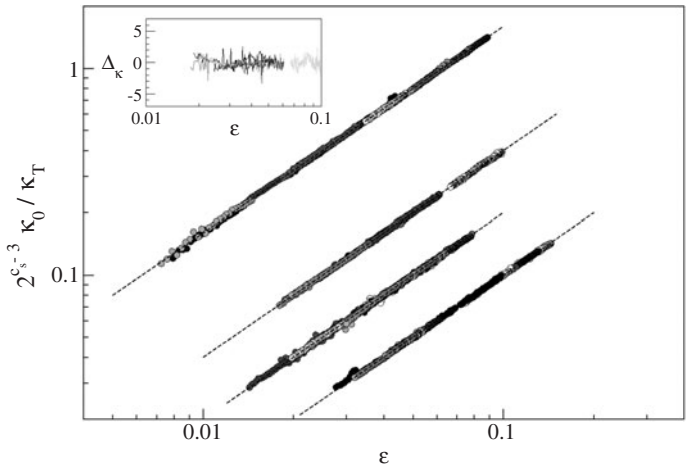

Figure 1. Scaling of the isothermal compressibility κ_T at different protein and salt concentrations. Solid lines are linear fits to data. NaCl concentration (from top to bottom): 7, 5, 4, 3% w/v. The factor $f = 2^{c_s-3}$, where c_s is the salt concentration in % w/v, has been used to visually separate the salt concentrations. Protein volume fractions at NaCl 7% w/v: $\phi = 0.039, 0.040, 0.051, 0.065, 0.076, 0.079, 0.091, 0.097, 0.118, 0.096, 0.097, 0.119$; at NaCl 5% w/v: $\phi = 0.032, 0.056, 0.075, 0.087, 0.109, 0.110, 0.119, 0.138$; at NaCl 4% w/v: $\phi = 0.027, 0.038, 0.036, 0.036, 0.048, 0.049, 0.050, 0.079, 0.064, 0.085, 0.097, 0.108, 0.109, 0.113, 0.127$; at NaCl 3% w/v: $\phi = 0.042, 0.049, 0.085, 0.99, 0.126, 0.115$. Inset: the percentual error of data at 5% NaCl, $\Delta_\kappa = 100(\kappa_T/\kappa_0 - \epsilon)/\epsilon$.

analogous to the present one. The same set-up has also been used to determine the correlation length of critical fluctuations (as we shall see in the next section) [14, 44–46].

In figure 1, scattered intensity experimental data (also reported in [25]) are plotted in the form of equation (1) with $\gamma = 1$, in order to show the scaling behaviour of the isothermal compressibility. Spinodal temperatures obtained from this scaling are plotted in figure 2.

Determination of the spinodal line can be very useful for modelling protein–protein interactions in solution. Indeed, an ansatz on the interaction potential can in many cases allow calculation of an analytic expression for the isothermal compressibility, and therefore for the spinodal line ($\kappa_T^{-1} = 0$).

The existence of a liquid–liquid phase transition metastable with respect to solid–liquid coexistence in protein or colloidal solutions has been explained by modelling solute interactions through a short range attractive potential [4, 5, 8, 9, 11]. Short range interactions are important in determining some properties of such solutions, especially at low concentrations and high ionic strength [47–49], even if long range forces (van der Waals attraction, electrostatic repulsion etc) [50–52] and non-isotropic interaction [53, 54] can also contribute in determining the phase diagram.

The simplest model for taking into account excluded volume effect and screened short range interactions is that of a square well potential for a spherical particle with a hard core of diameter σ, and a range of interaction $\lambda\sigma$:

$$v_{sw}(r) = \begin{cases} \infty, & r < \sigma, \\ -u, & \sigma \leqslant r \leqslant \lambda\sigma, \\ 0, & r > \lambda\sigma. \end{cases} \tag{2}$$

In the limit of an infinitely narrow and deep well (adhesive hard spheres), and in the Percus–Yevick approximation, an explicit expression for the compressibility has been derived [55]:

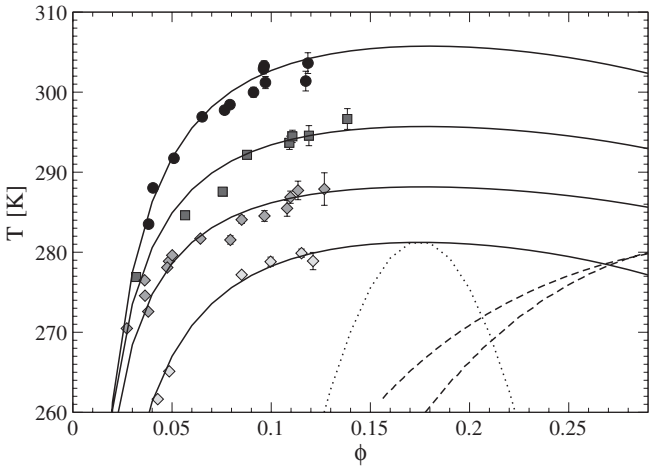

Figure 2. Spinodal points. Experimental data: NaCl 7% w/v (circles), 5% w/v (squares), 4% w/v (dark diamonds), 3% w/v (light diamonds). Solid curves are spinodal predictions obtained as described in the text for the extended adhesive hard sphere models (equations (3)–(7)); the values of the fitting parameters are $\lambda = 1.05$, $u = 0.72$ kcal mol^{-1} for all curves, and $h = 75, 85, 95, 65$ kcal mol^{-1}, $s = 0.24, 0.27, 0.32, 0.22$ kcal mol^{-1} K^{-1} respectively for [NaCl] = 7, 5, 4, 3% w/v. The dotted curve is a spinodal curve obtained within the same model, but with zero perturbative entropy ($s = 0$). Dashed curves are spinodal curves calculated in [11] using the SCOZA Yukawa potential with $b = 100$, $u = 4.16$ kcal mol^{-1} (upper curve) and $b = 30$, $u = 2.55$ kcal mol^{-1} (lower curve).

$$\frac{v_s}{\phi k_B T}\kappa_T^{-1} = \frac{(1 + 2\phi - 6b + \sqrt{36b^2 - 6G})^2}{(1-\phi)^4} \tag{3}$$

where ϕ is the volume fraction, v_s is the solute volume, $b = \tau(1-\phi) + \phi$, $G = 2\phi + \phi^2$ and

$$\tau^{-1} = \lim_{\substack{\lambda\to 1 \\ u\to\infty}} 12\frac{\lambda - 1}{\lambda} e^{\beta u}. \tag{4}$$

The so-called stickiness parameter τ indicates the deviation of the second virial coefficient B_2 from that for hard spheres: $B_2/B_2^{HS} = 1 - (4\tau)^{-1}$. The same expression for compressibility holds for a square well potential to zero order in $(1 - \lambda^{-1})$ [56], with an appropriate mapping of stickiness into square well parameters:

$$\tau^{-1} = 4(\lambda^3 - 1)(e^{\beta u} - 1). \tag{5}$$

It is worth noting that the easier choice of a hard sphere potential without an attractive part, that can be worked out to obtain an explicit equation for the compressibility (PY approximation [57], Carnahan–Starling formula [58]), would have been insufficient for reproducing the present and previous experimental results for the lysozyme critical volume fraction [13, 17, 20, 21, 25].

However, neither adhesive hard sphere expression for the compressibility (equation (3)) was sufficient to fit our spinodal points. A possible extension of the AHS model is based on standard perturbation theories [57]. Weak or long range interactions can be treated as a perturbation with respect to a reference potential which is explicitly considered in all calculations. By taking adhesive hard spheres as a reference system we can modify the compressibility equation to

$$\kappa_T^{-1} = \kappa_{T,0}^{-1} - 2a\phi^2, \tag{6}$$

where $\kappa_{T,0}$ denotes the reference compressibility (equation (3)), ϕ is the volume fraction and the parameter a represents the perturbation energy density per unit volume fraction. This parameter results from an averaging over many degrees of freedom; therefore, it is related to a free energy and can include both an energetic (or enthalpic) and an entropic term [59], following a classical approach from polymer physics [60]:

$$a = h - Ts. \tag{7}$$

Spinodal lines, calculated by equating to zero κ_T^{-1} in equation (6), are used to fit experimental data (figure 2). The same critical volume fraction has been used: $\phi_c = 0.177$, and $T_c = 32.5, 22.5, 15.0, 8.1\,^{\circ}\mathrm{C}$ respectively for [NaCl] = 7, 5, 4, 3% w/v. The value of λ has been fixed, reasonably, to 1.05, and the value of the potential u has been fixed to 0.72 kcal mol^{-1}. (Note that this is the same value as in [25], where it was misprinted.) This choice of parameters is quite critical to obtaining a reasonable value for the critical volume fraction, which was chosen as $\phi_c = 0.177$, according to [21] and to our data [25]. The curves are redrawn from [25], where an attempt to use a generalized van der Waals model was also discussed.

The necessity of including a perturbative term, and particularly the entropic part, arises from the positioning of the experimental spinodal temperatures which assumes a quite flat profile over volume fractions. (The dotted curve in figure 2 is drawn by assuming a zero entropic contribution, $s = 0$.) In order to improve our analysis, it is helpful to use an expression for compressibility calculated via the more refined self-consistent Ornstein–Zernike approximation (SCOZA) [61, 62, 11]. Calculations performed with this approach have given phase diagrams with metastable liquid–liquid coexistence and spinodal lines that look like good candidates for describing lysozyme solutions. As a first attempt, we plot in figure 2 (dashed curves) spinodal lines calculated in [11] for the SCOZA Yukawa potential for different values of the screening parameter b (roughly speaking, b is equiparable to the inverse of the range parameter in the square well potential, namely $[\lambda - 1]^{-1}$). Even if such curves have a larger extent than that calculated with the Baxter expression (equation (3) and the dotted curve in figure 2), the critical point is located at larger volume fractions, so they are not able to fit experimental data.

As a last comment, we note that it is reasonable that the model of hard spheres with short range attraction, appropriate for colloids in solutions, should be extended to globular proteins, which are complex objects of irregular shape and highly structured surface [53, 54, 63, 64], and with screened (yet long ranged) electrostatic interactions [65, 66]. The inclusion of an entropic term in the free energy was meant as an averaging over degrees of freedom including solvent molecules, so as to include the hydrophobic effect or hydration.

4. Slowing down

Isothermal compressibility diverges on approaching the spinodal line. From the fluctuation-dissipation theorem we learn that the compressibility is proportional to the amplitude of the concentration fluctuations [2, 42]. Also the correlation length and the relaxation time of concentration fluctuations are expected to diverge along with the compressibility on approaching instability. If the pseudospinodal hypothesis holds, the correlation length ξ should diverge critically on approaching the spinodal temperature:

$$\xi = \xi_0 \epsilon^{-\nu}, \tag{8}$$

where ν is a critical exponent related to the compressibility exponent γ by the equality $\gamma = 2\nu - \eta$ ($\eta = 0$ in the mean field) [42, 67].

By means of dynamic light scattering experiments, we have measured the relaxation rate Γ of the concentration fluctuations simultaneously with the isothermal compressibility. At each protein concentration, Γ decreases on approaching the spinodal temperature, and exhibits a remarkable linear correlation with κ_T^{-1}. Thus, we observed a slowing down related to the divergence of critical fluctuations on approaching instability at off-critical concentrations.

A typical observation in phase transition phenomena is the so-called 'critical slowing down'—that is, the divergence of the fluctuation relaxation time on approaching a second-order phase transition [42]. One of the first explanations of this slowing down comes from the relation between the relaxation rate of fluctuations Γ and the isothermal compressibility κ_T [40, 69]:

$$\Gamma = \frac{\alpha q^2}{\rho \kappa_T}. \tag{9}$$

In this expression, ρ is the number density, and the Onsager coefficient $\alpha = \alpha(T, \eta, \rho)$ is the concentration conductivity, supposed to have a very smooth dependence on temperature T and viscosity η [68].

If we maintain the assumption that α has no critical behaviour, Γ is expected to go to zero at the spinodal temperature with a linear dependence on the reduced temperature ϵ—that is, as the inverse compressibility: $\Gamma \sim \epsilon^{\gamma} \sim \epsilon^{2\nu}$.

On the other hand, if we consider concentration fluctuations of the correlation length ξ as liquid droplets of size ξ, we would expect from hydrodynamics the following expression (equivalent to the Stokes–Einstein equation for Brownian motion):

$$\Gamma = \frac{k_B T q^2}{6\pi\eta} \frac{1}{\xi}. \tag{10}$$

In this case, the critical behaviour of the relaxation rate should mirror that of the fluctuation correlation length: $\Gamma \sim \epsilon^{\nu}$.

Close to the critical point (or to the spinodal temperature), mode–mode coupling theory actually predicts expression (10) [42, 70]. However, not very close to instability, as in our experiments (where $\epsilon > 0.007$), a mean field approach would suggest the validity of expression (9) [71]. A more detailed calculation has been performed in the mode-coupling approach, considering transport coefficients as the sum of a critical and a background contribution [18, 44, 70–72]. In the OZ approximation, the relaxation rate is the sum of two contributions, corresponding respectively to equations (9) and (10) [73, 46]:

$$\Gamma = \frac{k_B T q^2}{6\pi\eta_0}\left[\frac{T_s \xi_c}{T\xi^2}(1+\xi^2 q^2) + \frac{1}{\xi}\frac{(1+\xi^2 q^2)^z}{(u\xi/\xi_c)^z K_0(\xi q)^{z-1}}\right] \tag{11}$$

where $\xi_c = [6\pi\eta_0\alpha_0/(\rho k_B T_s)]k_0^{-1}\xi_0^2$, α_0 and η_0 are respectively the background concentration conductivity and the background viscosity, ξ_0 and k_0 are the amplitude of the diverging correlation length and the compressibility (equations (1) and (8)) and $K_0(x) = 0.75x^{-2}[1 + x^2 + (x^3 - x^{-1})\arctan(x)]$ is the Kawasaki function [70]. The exponent z is related to the divergence of the viscosity ($\eta = \eta_0[u\xi/\xi_c]^z$), with $u \sim 0.675$ and $z \sim 0.054$ [73]. In the present experiments the correlation length is sufficiently small ($\xi q < 1$) that equation (11) can be simplified to the form [72]

$$\Gamma = \frac{k_B T q^2}{6\pi\eta_0}\left[\frac{T_s \xi_c}{T\xi^2} + \frac{1}{\xi}\right]. \tag{12}$$

Experimental data have been fitted using the latter equation and equation (8), with the critical exponent fixed at the mean field value $\nu = 0.5$ and the spinodal temperatures obtained from best fits of figure 1. We found a value for ξ_0 that increases with concentration as shown in

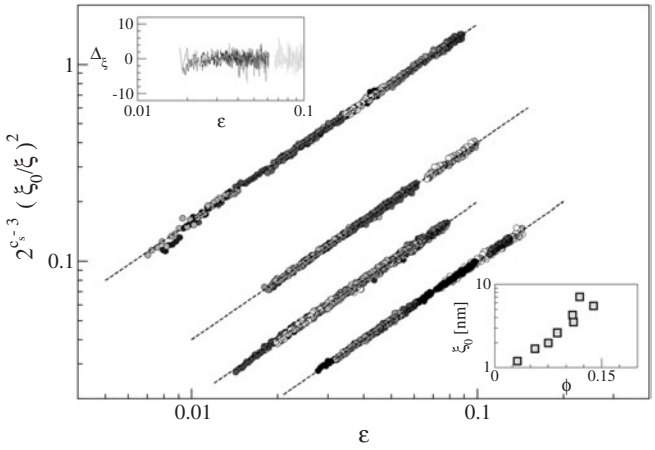

Figure 3. Scaling of correlation lengths at different salt and protein concentrations, obtained by taking into account both a critical and a background term ($\nu = 0.5$), as in equation (13). The factor $f = 2^{c_s-3}$, where c_s is the salt concentration in % w/v, has been used to visually separate the salt concentrations. Solid lines are linear fits to data. The NaCl and protein concentrations are as in figure 1. Upper inset: the percentual error of the data at 5% NaCl, $\Delta_\xi = 100(\xi_0^2/\xi^2 - \epsilon)/\epsilon$. Lower inset: the amplitude parameter ξ_0 of the data at 5% NaCl versus the volume fraction.

the inset of figure 3 (for one salt concentration, to avoid overcrowding the figure). As regards the parameter ξ_c, we found the expected dependence on ξ_0^2. By using fitting parameters and equation (12) the correlation length can be derived from the relaxation rate:

$$\xi = \xi^* \frac{1}{2}\left[1 + \sqrt{1 + \frac{4T_s\xi_c}{T\xi^*}}\right], \qquad \xi^* \equiv \frac{k_B T q^2}{6\pi\eta_0\Gamma}. \tag{13}$$

The scaling behaviour of the correlation length (according to the latter equation) is shown in figure 3.

As pointed out in [25], if we assume equation (10) to hold at any distance from the spinodal temperature, that is for any value of the reduced temperature ϵ, the data cannot be scaled by using a mean field exponent $\nu = 0.5$. Interestingly, a good scaling according to equation (8) is obtained by using a non-classical exponent $\nu = 0.63$, close to that obtained through renormalization group calculation at the critical point (figure 4). Moreover, in this case we obtain an amplitude parameter that is quite independent of volume fraction.

A clear explanation of these findings would of course require a more developed theory. A fact that seems robust with respect to all kinds of analyses is that the slowing down observed at off-critical concentration is actually due to (or at least strictly correlated with) the divergence of the amplitude of concentration fluctuation on approaching the region of liquid–liquid instability.

5. Conclusions

In the present work, we have reported static and dynamic light scattering experiments on a solution of lysozyme at pH 4.5 and at different ionic strengths (NaCl concentrations of 3, 4, 5 and 7% w/v). In our experimental conditions, lysozyme solutions are supersaturated and metastable with respect to the equilibrium coexistence between solid and liquid phases; on lowering the temperature they undergo a liquid–liquid phase transition [13, 17, 20–22].

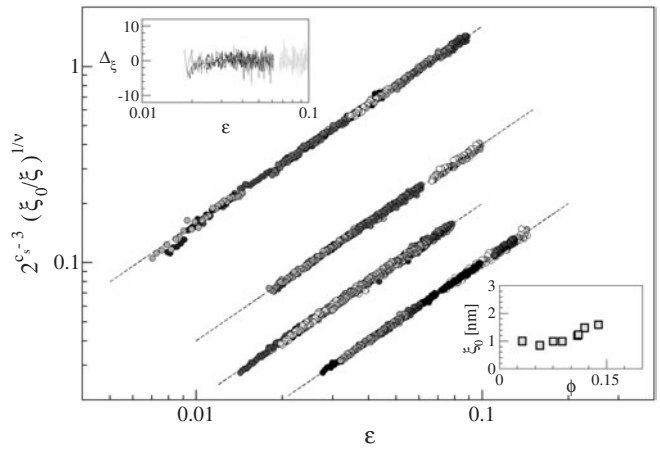

Figure 4. Scaling of correlation lengths at different salt and protein concentrations with a non-classical critical exponent ($\nu = 0.63$), obtained as in equation (10). The factor $f = 2^{c_s-3}$, where c_s is the salt concentration in % w/v, has been used to visually separate the salt concentrations. Solid lines are linear fits to data. The NaCl and protein concentrations are as in figure 1. Upper inset: the percentual error of the data at 5% NaCl, $\Delta_\xi = 100((\xi_0/\xi)^{1/\nu} - \epsilon)/\epsilon$. Lower inset: the amplitude parameter ξ_0 of the data at 5% NaCl versus the volume fraction.

The isothermal compressibility (related to the amplitude of the concentration fluctuations) has been found to diverge on approaching a given temperature [25]. This behaviour allows one to extrapolate the compressibility divergence to the spinodal temperatures, which mark the limit of stability. We show that the compressibility diverges following a power law (with an exponent $\gamma = 1$) on approaching the spinodal as it would do on approaching the critical point (the pseudospinodal hypothesis [35]).

Spinodal data can be interpreted with a model including excluded volume and short range interactions (adhesive hard spheres) as well as a perturbative term (perhaps mimicking long range interactions), with both an enthalpic and an entropic contribution, which, reasonably, takes into account the role of hydration water or a (mean field) hydrophobic effect.

The relaxation rate of concentration fluctuations determined by dynamic light scattering measurements goes to zero on approaching the spinodal line, with a strong correlation with the inverse compressibility. Here, we have addressed the possibility of measuring the correlation length of fluctuations from the relaxation rate within the framework of generalized hydrodynamics and mode-coupling theory [70, 73]. The slowing down of the dynamics observed at off-critical volume fractions is related to the scaling divergent behaviour of the correlation length.

Fluctuations close to the critical point have been shown to be relevant in enhancing the rate of crystal nucleation by providing droplets of high local concentration [36]. In this respect our experiments suggest that since off-critical fluctuations exhibit the same divergent scaling behaviour, they may have a key role in the crystallization mechanisms, as well as in the competition between crystal formation and dynamical structural arrest at higher concentration [74].

Acknowledgments

We thank F Sciortino and G Foffi for useful discussions and for sharing their data. One of the authors (MM) is indebted to G Stell for helpful and inspiring discussions.

References

[1] McPherson A 1999 *Crystallization of Biological Macromolecules* (Cold Spring Harbor, NY: Cold Spring Harbor Laboratory Press)
[2] Debenedetti P G 1996 *Metastable Liquids: Concepts and Principles* (Princeton, NJ: Princeton University Press)
[3] Baksh M M, Jaros M and Groves J T 2004 *Nature* **427** 139
[4] Gast A P, Russel W B and Hall C K 1983 *J. Colloid Interface Sci.* **96** 251
[5] Lekkerkerker H N W, Poon W C K, Pusy P N, Stroobants A and Warren P B 1992 *Europhys. Lett.* **20** 559
[6] Ilett S M, Orrock A, Poon W C K and Pusey P N 1995 *Phys. Rev.* E **51** 1344
[7] Poon W C K 2002 *J. Phys.: Condens. Matter* **14** R859
[8] Hagen M H J and Frenkel D 1994 *J. Chem. Phys.* **101** 4093
[9] Rosenbaum D, Zamora P C and Zukoski C F 1996 *Phys. Rev. Lett.* **76** 150
[10] Noro M G and Frenkel D 2000 *J. Chem. Phys.* **113** 2941
[11] Foffi G, McCullagh G D, Lawlor A, Zaccarelli E, Dawson K A, Sciortino F, Tartaglia P, Pini D and Stell G 2002 *Phys. Rev.* E **65** 031407
[12] George A and Wilson W W 1994 *Acta Crystallogr.* **50** 361
[13] Ishimoto C and Tanaka T 1977 *Phys. Rev. Lett.* **39** 474
[14] Schurtenberger P, Chamberlin R A, Thurston G M, Thomson J A and Benedek G B 1989 *Phys. Rev. Lett.* **63** 2064
[15] Broide M L, Berland C R, Pande J, Ogun O O and Benedek G B 1991 *Proc. Natl Acad. Sci. USA* **88** 5660
[16] Berland C R, Thurston G M, Kondo M, Broide M L, Pande J, Ogun O O and Benedek G B 1992 *Proc. Natl Acad. Sci. USA* **89** 1214
[17] Taratuta V G, Holschbach A, Thurston G M, Blankschtein D and Benedek G B 1990 *J. Phys. Chem.* **94** 2140
[18] Fine B M, Pande J, Lomakin A, Ogun O O and Benedek G B 1995 *Phys. Rev. Lett.* **74** 198
[19] Fine B M, Lomakin A, Ogun O O and Benedek G B 1996 *J. Chem. Phys.* **104** 326
[20] Broide M L, Tominc T M and Saxowsky M D 1996 *Phys. Rev.* E **53** 6325
[21] Mushol M and Rosenberger F 1997 *J. Chem. Phys.* **107** 1953
[22] Grigsby J J, Blanch H V and Prausnitz J M 2001 *Biophys. Chem.* **91** 231
[23] San Biagio P L and Palma M U 1991 *Biophys. J.* **60** 508
[24] San Biagio P L, Bulone D, Emanuele A and Palma M U 1996 *Biophys. J.* **70** 494
[25] Manno M, Xiao C, Bulone D, Martorana V and San Biagio P L 2003 *Phys. Rev.* E **68** 011904
[26] Evans R M L, Poon W C K and Cates M E 1997 *Europhys. Lett.* **38** 595
[27] Dixit N M, Kulkarni A M and Zukoski C F 2001 *Colloids Surf.* A **190** 47
[28] Drenth J and Haas C 1998 *Acta Crystallogr.* **54** 867
[29] Galkin O and Vekilov P G 2000 *Proc. Natl Acad. Sci. USA* **97** 6277
[30] Sear R P 2001 *Phys. Rev.* E **63** 66105
[31] Poon W C K 1997 *Phys. Rev.* E **55** 3762
[32] Bhamidi V, Skrzypczak-Jankun E and Schall C A 2001 *J. Cryst. Growth* **232** 77
[33] Georgalis Y, Umbach P, Soumpasis D M and Saenger W 1998 *J. Am. Chem. Soc.* **120** 5539
[34] Tanaka S, Ataka M and Ito K 2002 *Phys. Rev.* E **65** 051804
[35] Benedek G B 1969 *Polarisation, Matière et Rayonnement; Volume Jubilaire en l'Honneur d'Alfred Kastler* (Paris: Presses Universitaire de France)
[36] ten Wolde P R and Frenkel D 1997 *Science* **277** 1975
[37] Shen Y C and Oxtoby D W 1996 *J. Chem. Phys.* **104** 4233
[38] Talanquer V and Oxtoby D W 1998 *J. Chem. Phys.* **109** 223
[39] Sophianopoulos A J, Rhodes C K, Holcomb D N and Van Holde K 1962 *J. Biol. Chem.* **237** 1107
[40] Berne B J and Pecora R 1976 *Dynamic Light Scattering* (New York: Wiley–Interscience)
[41] Kirkwood J G and Oppenheim I 1961 *Chemical Thermodynamics* (New York: McGraw-Hill)
[42] Stanley H E 1971 *Introduction to Phase Transition and Critical Phenomena* (Oxford: Oxford University Press)
[43] Chu B, Schoenes F J and Fisher M E 1969 *Phys. Rev.* **185** 219
[44] Chen S H, Lai C C, Rouch J and Tartaglia P 1983 *Phys. Rev.* A **27** 1086
[45] Manno M, Emanuele A, Martorana V, San Biagio P L, Bulone D, Palma-Vittorelli M B, McPherson D T, Xu J, Parker T M and Urry D W 2001 *Biopolymers* **59** 51
[46] Burstyn H C and Sengers J W 1982 *Phys. Rev.* A **25** 448
[47] Kulkarni A and Zukoski C F 2001 *J. Cryst. Growth* **232** 156
[48] Piazza R, Peyre V and Degiorgio V 1998 *Phys. Rev.* E **58** R2733
[49] Malfois M, Bonneté F, Tardieu A and Belloni L 1996 *J. Chem. Phys.* **105** 3290
[50] Noro M G, Kern N and Frenkel D 1999 *Europhys. Lett.* **48** 332

[51] Sear R P 2000 *Phys. Rev.* E **61** 6019
[52] Pellicane G, Costa D and Caccamo C 2003 *J. Phys.: Condens. Matter* **15** 375
[53] Sear R P 1999 *J. Chem. Phys.* **111** 4800
[54] Lomakin A, Asherie N and Benedek G B 1999 *Proc. Natl Acad. Sci. USA* **96** 9465
[55] Baxter R J 1968 *J. Chem. Phys.* **49** 2770
[56] Chen W R, Chen S H and Mallamace F 2002 *Phys. Rev.* E **66** 021403
[57] Hansen J-P and McDonald I R 1986 *Theory of Simple Liquids* (San Diego, CA: Academic)
[58] Carnahan N F and Starling K E 1969 *J. Chem. Phys.* **51** 635
[59] Jansen J W, De Kruif C G and Vrij A 1984 *Chem. Phys. Lett.* **107** 450
[60] Flory P J 1953 *Principles of Polymer Chemistry* (Ithaca, NY: Cornell University Press)
[61] Pini D, Stell G and Wilding N B 1999 *Mol. Phys.* **95** 483
[62] Pini D, Stell G and Wilding N B 2001 *J. Chem. Phys.* **115** 2702
[63] Asherie N, Lomakin A and Benedek G B 1996 *Phys. Rev. Lett.* **77** 4832
[64] Lomakin A, Asherie N and Benedek G B 1996 *J. Chem. Phys.* **104** 1646
[65] Warren P B 2002 *J. Phys.: Condens. Matter* **14** 7617
[66] Allahyarov E, Lowen H, Hansen J-P and Louis A A 2003 *Phys. Rev.* E **67** 051404
[67] Fisher M E 1964 *J. Math. Phys.* **5** 944
[68] van Hove L 1954 *Phys. Rev.* **95** 1374
[69] Pusey P N 1991 *Liquid, Freezing and Glass Transition* ed J-P Hansen, D Levesque and J Zinn-Justin (Amsterdam: Elsevier Science)
[70] Kawasaki K 1970 *Ann. Phys.* **61** 1
[71] Swinney H L and Henry D L 1973 *Phys. Rev.* A **8** 2586
[72] Sorensen C M 1988 *J. Phys. Chem.* **92** 2367
[73] Oxtoby D W and Gelbart W M 1974 *J. Chem. Phys.* **61** 2957
[74] Zaccarelli E, Sciortino F, Tartaglia P, Foffi G, McCullagh G D, Lawlor A and Dawson K A 2002 *Physica* A **314** 539